

## Polyacetylenes from the roots of *Cirsium japonicum* var. *ussuriense*

Seung Hyun Lee<sup>a,1</sup>, Jun Gu Kim<sup>a,1</sup>, Thi Phuong Linh Le<sup>a</sup>, Jae Sang Han<sup>a</sup>, Yong Beom Cho<sup>a</sup>,  
Mi Kyeong Lee<sup>a</sup>, Dongho Lee<sup>b</sup>, Bang Yeon Hwang<sup>a,\*</sup>

<sup>a</sup> College of Pharmacy, Chungbuk National University, Cheongju, 28610, Republic of Korea

<sup>b</sup> Department of Biosystems and Biotechnology, College of Life Sciences and Biotechnology, Korea University, Seoul, 02841, Republic of Korea

### ARTICLE INFO

#### Keywords:

*Cirsium japonicum* var. *ussuriense*  
Asteraceae  
Polyacetylene  
Structure elucidation  
Nitric oxide

### ABSTRACT

Eight previously undescribed polyacetylenes, cirussurynes A-H, were isolated from the methanolic extract of the roots of *Cirsium japonicum* var. *ussuriense*. Their structures were elucidated by interpretation of extensive 1D and 2D NMR spectroscopy and HRESIMS spectrometry data. The configuration of triols in cirussurynes A, B, and E-G was deduced by the *J*-value based configuration analysis together with specific rotation values. All compounds were evaluated for their inhibitory effects on nitric oxide production against LPS-induced RAW 264.7 macrophages, and exhibited IC<sub>50</sub> values ranging from 5.5 to 68.7 μM.

### 1. Introduction

A perennial herbaceous plant that belongs to the family Asteraceae, *Cirsium japonicum* var. *ussuriense* (Regel) Kitam. ex Ohwi (synonym *Cirsium japonicum* var. *maackii* (Maxim.) Matsum.), is widely distributed in Korea, mainland China, and Japan. The roots of this plant exhibit a variety of biological activities, including anti-inflammatory, analgesic, and antipyretic properties (Kim, 1989; Bae, 2000; Park et al., 2004). Despite the ethnopharmacological significance of *C. japonicum* var. *ussuriense*, its chemical composition has rarely been investigated. Previous phytochemical investigations have revealed the presence of flavonoids and polyacetylenes in this plant. (Jeong et al., 2008; Kang et al., 2011; Thao et al., 2011; Shim et al., 2012; Park et al., 2017; Han et al., 2018).

Macrophages are known as the major cells involved in the inflammatory response by regulating various inflammatory mediators, such as pro-inflammatory cytokines, nitric oxide (NO), and tumor necrosis factor-α. Among these mediators, NO is a highly reactive substance, which is synthesized from L-arginine by NO synthase (NOS). NOS is classified as constitutive NOS (cNOS) and inducible NOS (iNOS). In particular, the expression of iNOS in various cells occurs upon stimulation by inflammatory cytokines and leads to the production of a large amount of NO (Cinelli et al., 2020). Therefore, the discovery of NO production inhibitors is expected to contribute to the treatment of inflammatory diseases (Kumar et al., 2017).

In a continuing search for the discovery of new anti-inflammatory constituents in traditional Korean medicinal plants, we found that *n*-hexane and CH<sub>2</sub>Cl<sub>2</sub>-soluble fractions from the MeOH extract of the roots of *C. japonicum* var. *ussuriense* possess inhibitory effects against LPS-induced NO production. Bioassay-guided separation of the *n*-hexane and CH<sub>2</sub>Cl<sub>2</sub>-soluble fractions led to the isolation of eight previously undescribed polyacetylenes (Fig. 1). Herein, details of the isolation and structure determination of the new compounds (1–8) as well as their inhibitory effects against NO production in LPS-induced RAW 264.7 macrophages are described.

### 2. Results and discussion

#### 2.1. Structure determination of the previously undescribed polyacetylenes

Compound 1 was obtained as a brown syrup. Its molecular formula was established as C<sub>17</sub>H<sub>24</sub>O<sub>3</sub> based on the <sup>13</sup>C NMR and HRESIMS data (*m/z* 299.1617 [M + Na]<sup>+</sup>, calcd 299.1618), indicating six degrees of unsaturation. The IR spectrum exhibited the characteristic absorptions of hydroxy group (3370 cm<sup>-1</sup>), conjugated acetylene (2296 cm<sup>-1</sup>), and terminal vinylic (1641, 912 cm<sup>-1</sup>) functionalities. The UV absorptions at 213, 266, and 283 nm suggested the presence of a polyacetylene moiety (Tsukamoto et al., 1997). The <sup>13</sup>C NMR and HSQC spectra of compound 1 showed 17 carbon signals, comprising a methyl group, five methylene carbons, three oxymethine carbons, two olefinic carbons at δ<sub>C</sub> 144.0

\* Corresponding author.

E-mail address: [byhwang@chungbuk.ac.kr](mailto:byhwang@chungbuk.ac.kr) (B.Y. Hwang).

<sup>1</sup> These authors equally contributed to the work.

(C-16) and 108.6 (C-15), a terminal vinylic group at  $\delta_C$  139.0 (C-2) and 114.3 (C-1), and four non-protonated alkyne carbons at  $\delta_C$  80.0 (C-11), 77.2 (C-13), 76.5 (C-14), and 72.0 (C-12) (Table 1). The  $^1\text{H}$  NMR spectrum of compound **1** revealed the presence of a *cis*-olefinic group at  $\delta_H$  6.16 (1H, dq,  $J = 10.8, 7.0$  Hz, H-16) and 5.51 (1H, d,  $J = 10.8$  Hz, H-15) and three oxygenated methine protons at  $\delta_H$  4.65 (1H, d,  $J = 3.8$  Hz, H-10), 4.05 (1H, m, H-8), and 3.56 (1H, dd,  $J = 3.5, 2.5$  Hz, H-9) (Table 1). The HMBC correlations of H-8 ( $\delta_H$  4.05)/C-6 ( $\delta_C$  25.3), C-7 ( $\delta_C$  33.7), C-9 ( $\delta_C$  74.3), C-10 ( $\delta_C$  66.3), H-9 ( $\delta_H$  3.56)/C-11 ( $\delta_C$  80.0), and H-10 ( $\delta_H$  4.65)/C-8 ( $\delta_C$  71.5), C-9 ( $\delta_C$  74.3), C-11 ( $\delta_C$  80.0), C-12 ( $\delta_C$  72.0) suggested the presence of triol groups at C-8, C-9, and C-10 (Fig. 2). This was further confirmed by the COSY correlations of H-8, H-9, and H-10 (Fig. 2). In addition, the HMBC correlations of H-15/C-13, C-14, C-16, C-17; and H-16/C-14, C-15, C-17 suggested the presence of a diyne-ene unit between C-11 and C-16 (Fig. 2). The relative configuration of compound **1** was assigned by Murata's method of  $J$ -value based configuration analysis (Matsumori et al., 1999). The most important part of this method is obtaining the precise values of the heteronuclear coupling constant between proton and carbon, therefore, the HETLOC, and HSQC-HECADE experiments were conducted to get the accurate measurement of coupling constants (Kozmiński and Nanz, 2000; Mence, 2008). The measured values of  $^3J$  (H-8, H-9),  $^3J$  (H-8, C-10),  $^3J$  (C-7, H-9),  $^2J$  (C-8, H-9), and  $^2J$  (C-9, H-8) matched well with the A-1 form among six staggered rotamers in Murata's method (Matsumori et al., 1999). Additionally, the set of  $J$ -values between C-9 and C-10 matched well with the B-2 form (Table 2). To clarify the absolute configuration of **1**, ECD calculation was performed using the same method used in a

previous study (Lai et al., 2014); however, the calculated data were insufficient to determine the absolute configuration (Wavefunction Inc., 2013). Therefore, the absolute configuration of C-8/C-9/C-10 can be assigned as *8R*/*9S*/*10R* or *8S*/*9R*/*10S*, and these two forms revealed the opposite specific rotation values in previous reports (Takaishi et al., 1990, 1991; Baek et al., 1995). Consequently, the absolute configuration of triol was assigned as *8S*/*9R*/*10S* from the observed positive specific rotation value ( $[\alpha]_D^{25} = +4$ ,  $c$  0.1, in MeOH). From these, the structure of compound **1** was determined as (+)-(8*S*,9*R*,10*S*,*Z*)-heptadeca-1,15-diene-11,13-diyne-8,9,10-triol, and named as cirussurynone A.

Compound **2** was obtained as a brown syrup. Its molecular formula was established as  $\text{C}_{17}\text{H}_{28}\text{O}_3$  based on the  $^{13}\text{C}$  NMR and HRESIMS data ( $m/z$  303.1931 [ $\text{M} + \text{Na}$ ] $^+$ , calcd 303.1931), indicating four degrees of unsaturation. The  $^1\text{H}$  and  $^{13}\text{C}$  NMR data were similar to those of compound **1**, except for the large coupling constant of the *trans*-olefinic group [ $\delta_H$  6.15 (1H, dt,  $J = 15.9, 7.2$  Hz, H-14), 5.47 (1H, d,  $J = 15.9$  Hz, H-13)], and two non-protonated alkyne carbons [ $\delta_C$  86.4 (C-12) and 84.8 (C-11)] (Table 1). The COSY correlations of the oxymethine protons revealed the same spin system of 8, 9, 10-triol (Fig. 2). The HMBC correlations of H-9 ( $\delta_H$  3.52)/C-11 ( $\delta_C$  84.8), H-10 ( $\delta_H$  4.63)/C-11 ( $\delta_C$  84.8), C-12 ( $\delta_C$  86.4), H-13 ( $\delta_H$  5.47)/C-11 ( $\delta_C$  84.8), C-12 ( $\delta_C$  86.4), C-14 ( $\delta_C$  146.4), C-15 ( $\delta_C$  35.1), and H-14 ( $\delta_H$  6.15)/C-12 ( $\delta_C$  86.4), C-15 ( $\delta_C$  35.1), C-16 ( $\delta_C$  21.8) suggested that the yne-ene (alkyne  $\text{C}\equiv\text{C}$  triple bond and alkene  $\text{C}=\text{C}$  double bond) unit is placed between C-11 and C-14 (Fig. 2). The  $J$ -value based configuration analysis was applied to compound **2** as well, and the same sets of  $^3J_{\text{H,H}}$ ,  $^3J_{\text{C,H}}$ ,  $^2J_{\text{C,H}}$  matched well with the A-1 form between C-8 and C-9, and the B-2 form between C-9

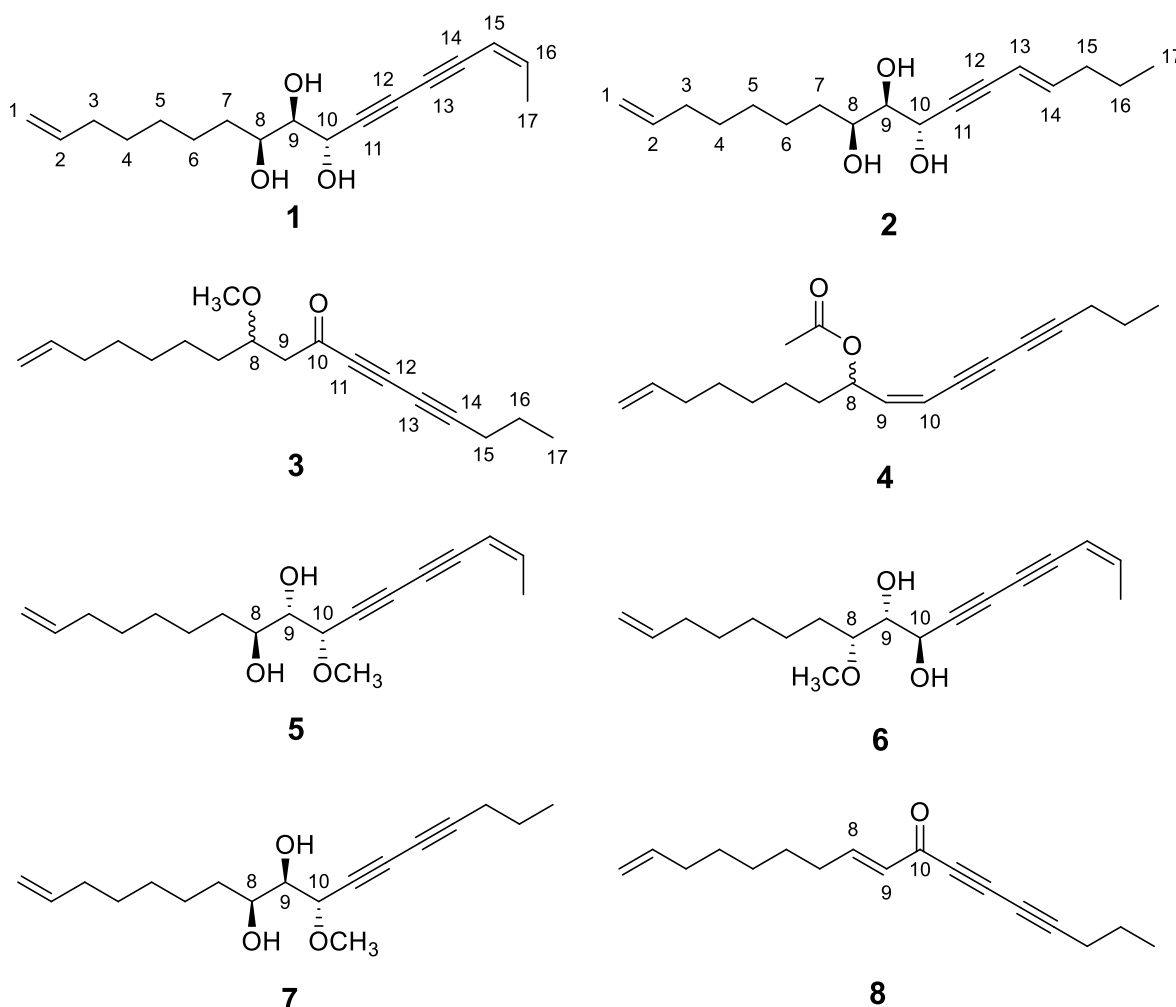


Fig. 1. Structures of compounds 1–8.

**Table 1**  
 $^1\text{H}$  and  $^{13}\text{C}$  NMR spectroscopic data for 1–4 in  $\text{CDCl}_3^{\text{d}}$ .

Carbon No.	1 <sup>b</sup>		2 <sup>c</sup>		3 <sup>d</sup>		4 <sup>e</sup>	
	$\delta_{\text{H}}$	$\delta_{\text{C}}$	$\delta_{\text{H}}$	$\delta_{\text{C}}$	$\delta_{\text{H}}$	$\delta_{\text{C}}$	$\delta_{\text{H}}$	$\delta_{\text{C}}$
1a	4.97 dd (17.1, 1.8)	114.3	4.97 dd (17.2, 2.0)	108.5	4.98 dd (17.1, 1.8)	114.3	4.98 dd (17.2, 1.7)	114.3
1b	4.92 dd (10.2, 1.8)		4.92 dd (10.2, 2.0)		4.93 dd (10.2, 1.9)		4.93 dd (10.2, 1.7)	
2	5.76 ddt (17.1, 10.2, 6.8)	139.0	5.77 ddt (17.1, 10.2, 6.8)	139.0	5.76 ddt (17.1, 10.2, 6.8)	139.0	5.78 ddt (17.1, 10.2, 6.8)	139.0
3	2.03 q (7.0)	33.7	2.03 q (6.9)	33.7	2.03 q (6.9)	33.7	2.03 q (6.9)	33.7
4	1.3–1.7 m	28.9	1.3–1.7 m	33.7	1.2–1.7 m	28.8	1.2–1.6 m	28.7
5	1.3–1.7 m	28.8	1.3–1.7 m	29.0	1.2–1.7 m	29.1	1.2–1.6 m	28.8
6	1.3–1.7 m	25.3	1.3–1.7 m	28.8	1.2–1.7 m	24.9	1.2–1.6 m	24.6
7	1.3–1.7 m	33.7	1.3–1.7 m	25.3	1.2–1.7 m	33.8	1.2–1.6 m	34.1
8	4.05 m	71.5	4.03 m	71.2	3.75 m	77.0	5.63 q (7.5)	72.8
9	3.56 dd (3.5, 2.5)	74.3	3.52 dd (3.9, 2.4)	74.5	2.61 dd (15.7, 7.5) 2.79 dd (15.7, 7.5)	50.1	5.90 dd (11.1, 7.5)	143.9
10	4.65 d (3.8)	66.3	4.63 d (3.8)	66.1		185.4	5.60 d (11.1)	110.3
11		80.0		84.8		72.4		70.3
12		72.0		86.4		76.7		80.5
13		77.2	5.47 d (15.9)	114.3		64.0		65.1
14		76.5	6.15 dt (15.9, 7.2)	146.4		91.0		86.1
15	5.51 d (10.8)	108.6	2.09 q (7.1)	35.1	2.35 t (6.9)	21.6	2.30 t (7.0)	21.6
16	6.16 dq (10.8, 7.0)	144.0	1.36 m	21.8	1.60 m	21.4	1.60 m	21.7
17	1.92 dd (6.9)	16.6	0.89 t (7.4)	13.6	1.01 t (7.4)	13.4	0.99 t (7.4)	13.5
$\text{OCH}_3$					3.34 s	57.1		
Acetyl $\text{CH}_3$							2.05 s	21.2
Acetyl CO								170.2

<sup>a</sup> The assignments were supported by HSQC and HMBC experiments.

<sup>b</sup>  $^1\text{H}$ -NMR, 400 MHz;  $^{13}\text{C}$ -NMR, 100 MHz.

<sup>c</sup>  $^1\text{H}$ -NMR, 400 MHz;  $^{13}\text{C}$ -NMR, 100 MHz.

<sup>d</sup>  $^1\text{H}$ -NMR, 900 MHz;  $^{13}\text{C}$ -NMR, 225 MHz.

<sup>e</sup>  $^1\text{H}$ -NMR, 800 MHz;  $^{13}\text{C}$ -NMR, 200 MHz.

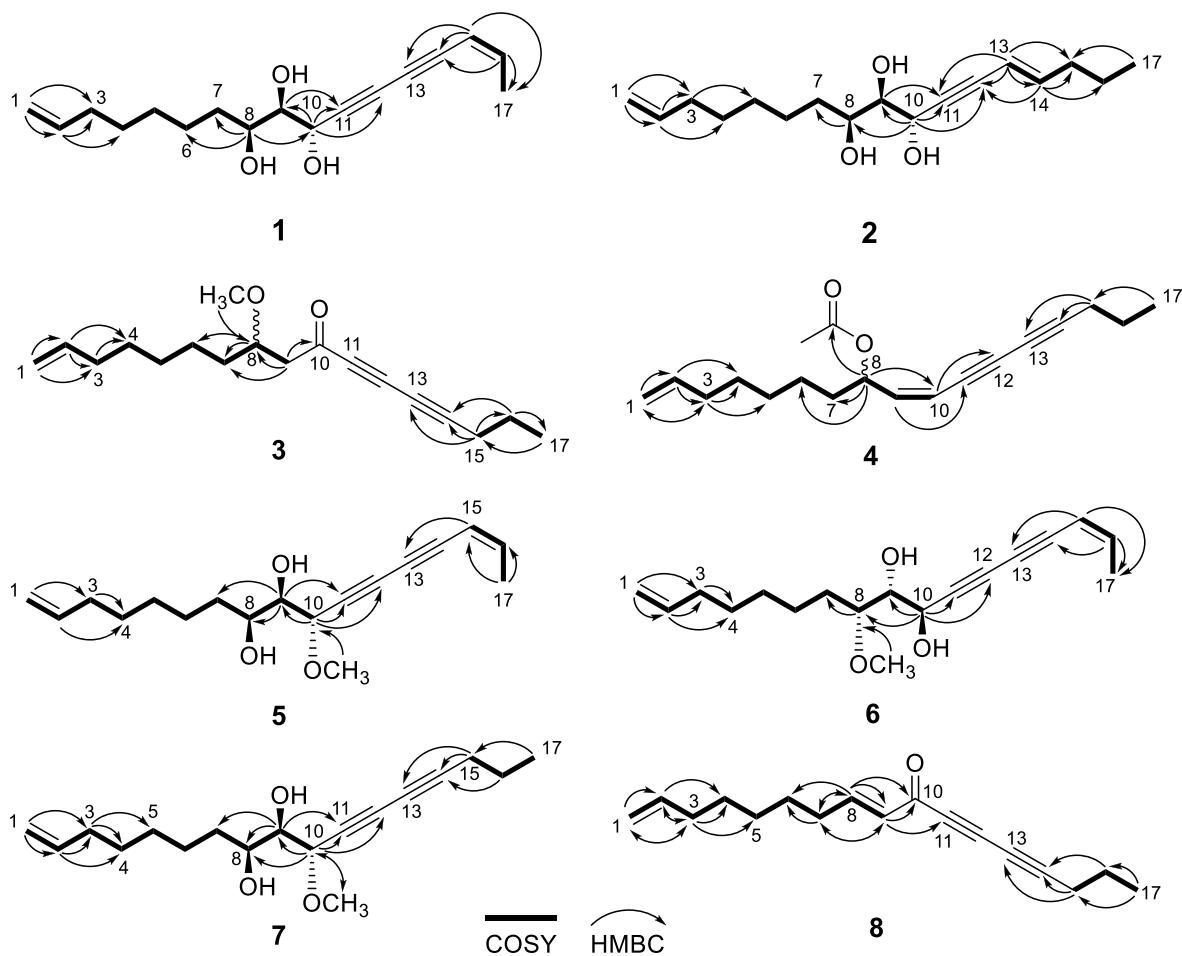
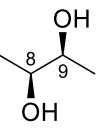
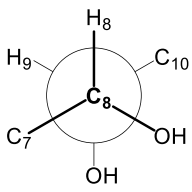
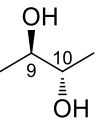
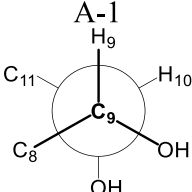


Fig. 2. Key HMBC and COSY correlations of compounds 1–8.

**Table 2**  
J-value based configuration analysis of the C8–C9 and C9–C10 segments of compounds **1** and **2**.

segment	$^{2,3}J_{\text{HX}}$	nuclei	value (Hz) <sup>a</sup>		magnitude estimation	rotamer (configuration)
			1	2		
 C8–C9	$^3J_{\text{HH}}$	H8–H9	2.5	2.4	small	 A-1
	$^3J_{\text{HC}}$	H8–C10	2.2	1.8	small	
		C7–H9	2.5	2.1	small	
	$^2J_{\text{HC}}$	C8–H9	0.8	0.3	small	
		C9–H8	0.8	1.1	small	
 C9–C10	$^3J_{\text{HH}}$	H9–H10	3.8	3.8	small	 B-2
	$^3J_{\text{HC}}$	H9–C11 <sup>b</sup>	–	–	–	
		C8–H10	3.8	4.5	large	
	$^2J_{\text{HC}}$	C9–H10	4.8	5.0	large	
		C10–H9	1.0	1.0	small	

<sup>a</sup> The values of the heteronuclear coupling constant were obtained by HETLOC and HSQC-HECADE experiments.

<sup>b</sup>  $^3J_{\text{(H-9,C-11)}}$  could not be obtained.

and C-10, implying the configuration of 8R/9S/10R or 8S/9R/10S (Table 2). As in compound **1**, the absolute configuration of triol in compound **2** was determined as 8S/9R/10S from the observed positive specific rotation value ( $[\alpha]_{\text{D}}^{25} = +3$ ,  $c$  0.1, in MeOH). Thus, the structure of compound **2** was determined as (+)-(8S,9R,10S,E)-heptadeca-1,13-diene-11-yne-8,9,10-triol, and named as cirussuryne B.

Compounds **3** was obtained as a brown syrup. Its molecular formula was established as  $\text{C}_{18}\text{H}_{26}\text{O}_2$  based on the  $^{13}\text{C}$  NMR and HRESIMS data ( $m/z$  297.1828 [ $\text{M} + \text{Na}$ ]<sup>+</sup>, calcd 297.1825), indicating six degrees of unsaturation. The IR spectrum exhibited the characteristic absorptions of carbonyl ( $1745\text{ cm}^{-1}$ ), conjugated acetylene ( $2298\text{ cm}^{-1}$ ), and terminal vinylic ( $1643, 904\text{ cm}^{-1}$ ) functionalities. The  $^{13}\text{C}$  NMR and HSQC spectra of **3** showed 18 carbon signals assigned to a methyl, eight methylenes, an oxymethine, a terminal vinylic group [ $\delta_{\text{C}}$  139.0 (C-2) and 114.3 (C-1)], four non-protonated alkynes [ $\delta_{\text{C}}$  91.0 (C-14), 76.7 (C-12), 72.4 (C-11), and 64.0 (C-13)], a carbonyl carbon [ $\delta_{\text{C}}$  185.4 (C-10)], and a methoxy carbon [ $\delta_{\text{C}}$  57.1 (8-OCH<sub>3</sub>)] (Table 1). The  $^1\text{H}$  NMR spectrum of **3** revealed the presence of an oxygenated methine proton at  $\delta_{\text{H}}$  3.75 (H-8) and a downfield-shifted methylene [ $\delta_{\text{H}}$  2.79 (H-9a) and 2.61 (H-9b)] (Table 1). The HMBC correlations of H-8 ( $\delta_{\text{H}}$  3.75)/C-6 ( $\delta_{\text{C}}$  24.9), C-7 ( $\delta_{\text{C}}$  33.8), C-9 ( $\delta_{\text{C}}$  50.1), C-10 ( $\delta_{\text{C}}$  185.4), 8-OCH<sub>3</sub> ( $\delta_{\text{C}}$  57.1), and H-9 ( $\delta_{\text{H}}$  2.61 and 2.79)/C-7 ( $\delta_{\text{H}}$  33.8), C-8 ( $\delta_{\text{C}}$  77.0), C-10 ( $\delta_{\text{C}}$  185.4), C-11 ( $\delta_{\text{C}}$  72.4) confirmed that a methoxy group is connected to C-8 and a carbonyl group is located at C-10 (Fig. 2). Based on the COSY correlations of H-1a ( $\delta_{\text{H}}$  4.98) and H-1b ( $\delta_{\text{H}}$  4.93)/H-2 ( $\delta_{\text{H}}$  5.76), H-2 ( $\delta_{\text{H}}$  5.76)/H-3 ( $\delta_{\text{H}}$  2.03), H-8 ( $\delta_{\text{H}}$  3.75)/H-9 ( $\delta_{\text{H}}$  2.61 and 2.79), H-15 ( $\delta_{\text{H}}$  2.35)/H-16 ( $\delta_{\text{H}}$  1.60), and H-16 ( $\delta_{\text{H}}$  1.60)/H-17 ( $\delta_{\text{H}}$  1.01), the carbonyl group was verified to be located at C-10 and two alkyne groups were assigned to C-11 through C-14 (Fig. 2). Thus, the structure of **3** was determined as (–)-heptadeca-1-ene-11,13-diyne-8-methoxy-10-one, and named as cirussuryne C.

Compound **4** was isolated as a brown syrup. Its molecular formula was established as  $\text{C}_{19}\text{H}_{26}\text{O}_2$  from the  $^{13}\text{C}$  NMR and HRESIMS data ( $m/z$

309.1823 [ $\text{M} + \text{Na}$ ]<sup>+</sup>, calcd 309.1825), indicating seven degrees of unsaturation. The 1D NMR data of **4** were similar to those of **3**, except for the absence of a carbonyl and methoxy group, and the presence of olefinic [ $\delta_{\text{C}}$  143.9 and 110.3;  $\delta_{\text{H}}$  5.90 (1H, dd,  $J = 11.1$  and 7.5 Hz, H-9) and 5.60 (1H, d,  $J = 11.1$  Hz, H-10)] and acetyl group [ $\delta_{\text{C}}$  170.2 (C=O) and 21.2 (O=C–CH<sub>3</sub>);  $\delta_{\text{H}}$  2.05 (3H, s, O=C–CH<sub>3</sub>)]. The HMBC correlations of H-8 ( $\delta_{\text{H}}$  5.63)/C-6 ( $\delta_{\text{C}}$  24.6), C-7 ( $\delta_{\text{C}}$  34.1), C-9 ( $\delta_{\text{C}}$  143.9), C-10 ( $\delta_{\text{C}}$  110.3), and 8-acetyl C=O ( $\delta_{\text{C}}$  170.2) confirmed that the acetyl group is located at C-8. The COSY correlations of H-1a ( $\delta_{\text{H}}$  4.98) and H-1b ( $\delta_{\text{H}}$  4.93)/H-2 ( $\delta_{\text{H}}$  5.78), H-2 ( $\delta_{\text{H}}$  5.78)/H-3 ( $\delta_{\text{H}}$  2.03), H-7 ( $\delta_{\text{H}}$  1.2, 1.6)/H-8 ( $\delta_{\text{H}}$  5.63), H-8 ( $\delta_{\text{H}}$  5.63)/H-9 ( $\delta_{\text{H}}$  5.90), H-9 ( $\delta_{\text{H}}$  5.90)/H-10 ( $\delta_{\text{H}}$  5.60), H-15 ( $\delta_{\text{H}}$  2.30)/H-16 ( $\delta_{\text{H}}$  1.60), and H-16 ( $\delta_{\text{H}}$  1.60)/H-17 ( $\delta_{\text{H}}$  0.99), and the HMBC correlations of H-9 ( $\delta_{\text{H}}$  5.90)/C-7 ( $\delta_{\text{C}}$  34.1), C-10 ( $\delta_{\text{C}}$  110.3), C-11 ( $\delta_{\text{C}}$  70.3) and H-10 ( $\delta_{\text{H}}$  5.60)/C-8 ( $\delta_{\text{C}}$  72.8), C-9 ( $\delta_{\text{C}}$  143.9), C-12 ( $\delta_{\text{C}}$  80.5) indicated that the olefinic bond was located at C-9 and C-10 (Fig. 2). Additionally, the olefinic group was assigned as the Z configuration based on the vicinal coupling constant ( $J = 11.1$  Hz). Thus, the structure of **4** was determined as (+)-8-acetyloxy-(Z)-heptadeca-1,9-diene-11,13-diyne, and named as cirussuryne D.

Compounds **5** was obtained as a brown syrup. Its molecular formula was established as  $\text{C}_{18}\text{H}_{26}\text{O}_3$  based on the  $^{13}\text{C}$  NMR and HRESIMS data ( $m/z$  313.1772 [ $\text{M} + \text{Na}$ ]<sup>+</sup>, calcd 313.1774). Its molecular weight was 14 Da higher than that of **1**, indicating the presence of a methoxy group rather than that of a hydroxy group. The 1D NMR data of compound **5** was also similar to that of **1**, except for the presence of a methoxy group at C-10 [ $\delta_{\text{H}}$  3.49 (3H, s);  $\delta_{\text{C}}$  57.2] (Table 3). Furthermore, the HMBC correlations of H-9 ( $\delta_{\text{H}}$  3.68)/C-7 ( $\delta_{\text{C}}$  32.5), C-8 ( $\delta_{\text{C}}$  72.1), C-11 ( $\delta_{\text{C}}$  78.4), H-10 ( $\delta_{\text{H}}$  4.24)/C-9 ( $\delta_{\text{C}}$  75.6), C-11 ( $\delta_{\text{C}}$  78.4), C-12 ( $\delta_{\text{C}}$  72.7), 10-OCH<sub>3</sub> ( $\delta_{\text{C}}$  57.2), and 10-OCH<sub>3</sub> ( $\delta_{\text{H}}$  3.49)/C-10 ( $\delta_{\text{C}}$  72.6) confirmed that the methoxy group is attached to C-10 (Fig. 2). The configuration of triol was determined by J-value based configuration analysis, as in compounds **1** and **2**. In compound **5**, the coupling constants of  $^3J$  (H-8, H-9),  $^3J$  (H-8, C-10),  $^3J$  (C-7, H-9),  $^2J$  (C-8, H-9), and  $^2J$  (C-9, H-8) indicated

**Table 3**  
<sup>1</sup>H and <sup>13</sup>C NMR spectroscopic data for 5–8 in CDCl<sub>3</sub><sup>a</sup>.

Carbon No.	5 <sup>b</sup>		6 <sup>b</sup>		7 <sup>c</sup>		8 <sup>c</sup>	
	δ <sub>H</sub>	δ <sub>C</sub>	δ <sub>H</sub>	δ <sub>C</sub>	δ <sub>H</sub>	δ <sub>C</sub>	δ <sub>H</sub>	δ <sub>C</sub>
1a	4.98 dd (17.1, 2.0)	114.3	4.99 dd (17.1, 1.8)	114.4	4.98 dd (17.1, 1.6)	114.2	4.99 dd (17.1, 1.7)	114.5
1b	4.93 dd (10.2, 2.0)		4.94 dd (10.2, 1.8)		4.92 dd (10.2, 1.6)		4.94 dd (10.2, 1.7)	
2	5.79 ddt (17.0, 10.3, 6.8)	139.1	5.79 ddt (17.0, 10.2, 6.7)	138.9	5.78 ddt (17.1, 10.1, 6.8)	139.1	5.77 ddt (17.1, 10.2, 6.6)	138.8
3	2.04 q (7.0)	33.7	2.05 q (7.0)	33.7	2.04 q (6.9)	33.8	2.04 q (6.8)	33.6
4	1.2–1.7 m	28.8	1.2–1.7 m	28.8	1.3–1.6 m	28.8	1.2–1.6 m	28.6
5	1.2–1.7 m	29.0	1.2–1.7 m	29.3	1.3–1.6 m	29.0	1.2–1.6 m	28.6
6	1.2–1.7 m	25.6	1.2–1.7 m	24.9	1.3–1.6 m	25.6	1.2–1.6 m	27.7
7	1.2–1.7 m	32.5	1.2–1.7 m	29.2	1.3–1.6 m	32.5	2.28 q (7.0)	32.7
8	3.79 m	72.1	3.65 m	81.5	3.78 m	72.1	7.14 dt (15.8, 7.0)	155.2
9	3.68 t (5.3)	75.6	3.62 m (7.8, 4.4)	73.0	3.64 dd (5.1)	72.5	6.15 d (15.8)	132.3
10	4.24 d (5.5)	72.6	4.56 q (4.5)	65.7	4.15 d (5.6)	75.6		177.6
11		78.4		80.7		71.2		70.9
12		72.7		71.3		73.1		76.5
13		77.2		77.2		64.4		64.1
14		76.0		76.0		81.9		89.6
15	5.52 d (10.9)	108.6	5.52 d (10.8)	108.7	2.26 t (7.0)	21.2	2.35 t (7.0)	21.6
16	6.19 dq (10.9, 6.9)	143.9	6.17 dq (10.8, 7.0)	143.7	1.56 m	21.6	1.59 m	21.4
17	1.93 d (6.9)	16.9	1.92 d (7.0)	16.5	0.99 t (7.4)	13.5	1.01 t (7.5)	13.5
OCH <sub>3</sub>	3.49 s	57.2	3.44 s	57.4	3.47 s	57.0		

<sup>a</sup> The assignments were supported by HSQC and HMBC experiments.

<sup>b</sup> <sup>1</sup>H-NMR, 900 MHz; <sup>13</sup>C-NMR, 225 MHz.

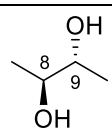
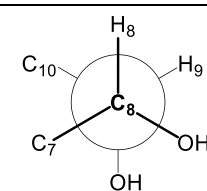
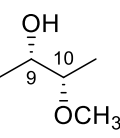
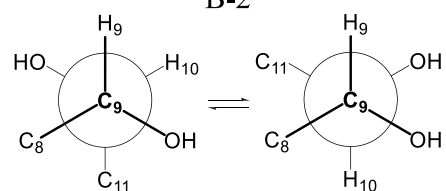
<sup>c</sup> <sup>1</sup>H-NMR, 700 MHz; <sup>13</sup>C-NMR, 175 MHz.

that the conformation of C-8 and C-9 matched well with the B-2 form, while <sup>3</sup>J (H-9, H-10), and <sup>3</sup>J (C-8, H-10) showed medium values, suggesting the presence of A-2 and A-3 transition conformers between C-9 and C-10. This analysis indicated that the configuration of triol can be 8R/9R/10R or 8S/9S/10S (Table 4), and it was assigned as 8S/9S/10S by positive specific rotation value ([α]<sub>D</sub><sup>25</sup> = +6, c 0.1, in MeOH). Thus, the structure of compound 5 was determined as (+)-(8S,9S,10S,Z)-10-methoxy-heptadeca-1,15-diene-11,13-diyne-8,9-diol, and named as

circussuryne E.

Compound 6 was obtained as a brown syrup. Its molecular formula was established as C<sub>18</sub>H<sub>26</sub>O<sub>3</sub>, the same as that of 5, based on the <sup>13</sup>C NMR and HRESIMS data (*m/z* 313.1773 [M + Na]<sup>+</sup>, calcd 313.1774). The <sup>1</sup>H, <sup>13</sup>C NMR, COSY, and HSQC spectra of 6 were similar to that of 5, except for the position of the methoxy group (Table 3). The HMBC correlations of H-8 (δ<sub>H</sub> 3.65)/C-7 (δ<sub>C</sub> 29.2), C-10 (δ<sub>C</sub> 65.7), 8-OCH<sub>3</sub> (δ<sub>C</sub> 57.4), 8-OCH<sub>3</sub> (δ<sub>H</sub> 3.44)/C-8 (δ<sub>C</sub> 81.5), and H-10 (δ<sub>H</sub> 4.56)/C-8 (δ<sub>C</sub> 81.5),

**Table 4**  
*J*-value based configuration analysis of the C8–C9 and C9–C10 segments of compound 5.

segment	<sup>2,3</sup> J <sub>HX</sub>	nuclei	value (Hz) <sup>a</sup>	magnitude estimation	rotamer (configuration)
 C8-C9	<sup>3</sup> J <sub>HH</sub>	H8–H9	3.8	small	 B-2
		<sup>3</sup> J <sub>HC</sub>	H8–C10	3.6	
	<sup>2</sup> J <sub>HC</sub>	C7–H9	10.9	large	
		C8–H9	5.0	large	
		C9–H8	2.5	small	
 C9-C10	<sup>3</sup> J <sub>HH</sub>	H9–H10	5.5	medium	 A-2 ↔ A-3
		<sup>3</sup> J <sub>HC</sub>	H9–C11 <sup>b</sup>	–	
	<sup>2</sup> J <sub>HC</sub>	C8–H10	2.6	medium	
		C9–H10	4.7	large	
		C10–H9	5.6	large	

<sup>a</sup> The values of the heteronuclear coupling constant were obtained by HETLOC and HSQC-HECADE experiments.

<sup>b</sup> <sup>3</sup>J<sub>(H-9,C-11)</sub> could not be obtained.

C-9 ( $\delta_C$  73.0), C-11 ( $\delta_C$  80.7), C-12 ( $\delta_C$  71.3) confirmed that the methoxy group is connected to C-8 (Fig. 2). The absolute configuration of compound **6** was determined in the same manner as that of compound **5**. The *J*-value based configuration analysis obtained by the HETLOC and HSQC-HECADE experiments indicated A-1 conformation for C-8 and C-9 and the mixed conformation of B-2 and B-3 for C-9 and C-10, implying the configuration of either 8*R*/9*R*/10*R* or 8*S*/9*S*/10*S* (Table 5). The absolute configuration of **6** was determined as 8*R*/9*R*/10*R* by the observed negative specific rotation value ( $[\alpha]_D^{25} = -12$ , *c* 0.1, in MeOH). Thus, the structure of compound **6** was determined as (-)-(8*R*,9*R*,10*R*,*Z*)-8-methoxy-heptadeca-1,15-diene-11,13-diyne-9,10-diol, and named as cirussuryne F.

Compound **7** was obtained as a brown syrup. Its molecular formula was established as C<sub>18</sub>H<sub>28</sub>O<sub>3</sub> based on the <sup>13</sup>C NMR and HRESIMS data (*m/z* 315.1928 [M + Na]<sup>+</sup>, calcd 315.1931). The <sup>1</sup>H and <sup>13</sup>C NMR data of compound **7** were similar to those of **5**, except for the presence of a methylene group [ $\delta_H$  2.26 (2H, t, *J* = 7.0 Hz, H-15) and 1.56 (2H, m, H-16);  $\delta_C$  21.2 and 21.6] instead of a *cis*-olefinic group in **5** (Table 3). The *J*-value based configuration analysis of **7** indicated A-1 conformation for C-8 and C-9 and the mixed conformation of B-2 and B-3 for C-9 and C-10, suggesting the configuration of either 8*R*/9*S*/10*R* or 8*S*/9*R*/10*S* (Table 5). The positive specific rotation value of **7** ( $[\alpha]_D^{25} = +6$ , *c* 0.1, in MeOH) confirmed the absolute configuration of 8*S*/9*R*/10*S*. Thus, the structure of **7** was determined as (+)-(8*S*,9*R*,10*S*)-10-methoxy-heptadeca-1-ene-11,13-diyne-8,9-diol, and named as cirussuryne G.

Compound **8** was obtained as a brown syrup. Its molecular formula was established as C<sub>17</sub>H<sub>22</sub>O based on the <sup>13</sup>C NMR and HRESIMS data (*m/z* 265.1562 [M + Na]<sup>+</sup>, calcd 265.1563), indicating the presence of 7 degrees of unsaturation. The <sup>1</sup>H and <sup>13</sup>C NMR data of compound **8** were

similar to those of **3**, except for the presence of a *trans*-olefinic group [ $\delta_H$  7.14 (1H, dt, *J* = 15.8, 7.0 Hz, H-8), 6.15 (1H, d, *J* = 15.8 Hz, H-9);  $\delta_C$  155.2 and 132.3] instead of a methoxy group in **3** (Table 3). The HMBC correlations of H-7 ( $\delta_H$  2.28)/C-6 ( $\delta_C$  27.7), C-8 ( $\delta_C$  155.2), C-9 ( $\delta_C$  132.3), H-8 ( $\delta_H$  7.14)/C-6 ( $\delta_C$  27.7), C-7 ( $\delta_C$  32.7), C-9 ( $\delta_C$  132.3), C-10 ( $\delta_C$  177.6), and H-9 ( $\delta_H$  6.15)/C-7 ( $\delta_C$  32.7), C-10 ( $\delta_C$  177.6), C-11 ( $\delta_C$  70.9) confirmed that a carbonyl group is located at C-10 and the *trans*-olefinic proton was positioned between C-8 and C-9 (Fig. 2). Thus, the structure of **8** was determined as (*E*)-heptadeca-1,8-diene-11,13-diyne-10-one, and named as cirussuryne H.

## 2.2. Inhibitory effects on nitric oxide production

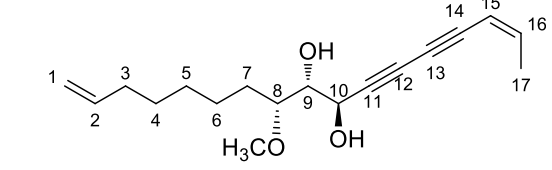
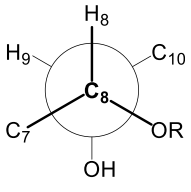
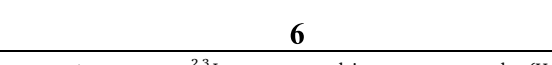
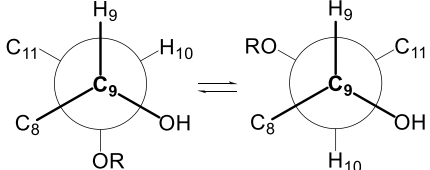
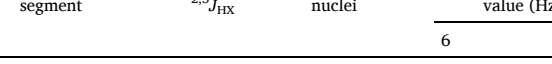
All compounds were evaluated for their inhibitory effects on LPS-induced NO production in RAW 264.7 macrophages using the Griess reaction. Aminoguanidine was used as a positive control (IC<sub>50</sub> = 20.6 μM) (Table 6). Cell viability was evaluated by an MTT assay, indicating

**Table 6**  
Inhibitory effects of compounds **1–8** on LPS-induced NO production in RAW 264.7 cells<sup>a</sup>.

Compound	IC <sub>50</sub> (μM) <sup>a</sup>	Compound	IC <sub>50</sub> (μM) <sup>a</sup>
<b>1</b>	13.4	<b>5</b>	7.6
<b>2</b>	44.0	<b>6</b>	9.7
<b>3</b>	5.5	<b>7</b>	68.7
<b>4</b>	17.8	<b>8</b>	6.1

<sup>a</sup> The results are expressed as mean IC<sub>50</sub> values from triplicate experiments. Aminoguanidine was used as the positive control (IC<sub>50</sub> = 20.6 μM).

**Table 5**  
*J*-value based configuration analysis of the C8–C9 and C9–C10 segments of compounds **6** and **7**.

segment	<sup>2,3</sup> <i>J</i> <sub>HX</sub>	nuclei	value (Hz) <sup>a</sup>		magnitude estimation	rotamer (configuration)
			<b>6</b>	<b>7</b>		
 <b>6</b>	<sup>3</sup> <i>J</i> <sub>HH</sub>	H8–H9	3.6	1.0	small	 A-1
		<sup>3</sup> <i>J</i> <sub>HC</sub>	H8–C10	1.1	3.5	
	<sup>2</sup> <i>J</i> <sub>HC</sub>	C7–H9	1.2	2.3	small	
		C8–H9	1.4	1.7	small	
 <b>6</b>	<sup>3</sup> <i>J</i> <sub>HH</sub>	H9–H10	4.4	5.1	medium	 B-2 ↔ B-3
		<sup>3</sup> <i>J</i> <sub>HC</sub>	H9–C11 <sup>b</sup>	–	–	
	<sup>2</sup> <i>J</i> <sub>HC</sub>	C8–H10	5.5	4.2	medium	
		C9–H10	5.0	4.7	medium	
 <b>7</b>	<sup>2</sup> <i>J</i> <sub>HC</sub>	C10–H9	1.9	2.7	large	

<sup>a</sup> The values of the heteronuclear coupling constant were obtained by HETLOC and HSQC-HECADE experiments.

<sup>b</sup> <sup>3</sup>*J*<sub>(H-9,C-11)</sub> could not be obtained.

that all test compounds showed no cytotoxicity to RAW 264.7 cells at their effective concentration range (data not shown). All polyacetylenes (1–8) suppressed NO production in LPS-induced RAW 264.7 cells with IC<sub>50</sub> values ranging from 5.5 to 68.7 μM. Compounds 3 and 8 exhibited potent inhibitory effects, with IC<sub>50</sub> values of 5.5 and 6.1 μM, respectively, suggesting that the presence of a carbonyl group adjacent to the diyne moiety seems to be crucial for NO inhibition. Compounds 1, 4, 5, and 6, which contain diene and diyne moieties, showed significant inhibitory effects, with IC<sub>50</sub> values of 13.4, 17.8, 7.6, and 9.7 μM, respectively. However, compounds 2 and 7 showed weak inhibitory effects with IC<sub>50</sub> values of 44.0 and 68.7 μM, respectively. These results implied that the conjugated diyne-ene moiety had a significant role in the NO inhibitory activity. Polyacetylenes, a class of secondary metabolites characterized by the presence of one or more carbon-carbon triple bonds in their structures, are commonly discovered in the members of Apiaceae, Asteraceae, Araliaceae, and Campanulaceae families (Chen et al., 2015; Negri, 2015). Polyacetylenes are well known to exhibit cytotoxic, antimicrobial, antifungal, and anti-inflammatory activities (Christensen, 2020). Some polyacetylenes from the Asteraceae family have been shown to inhibit NO production (Yao and Yang, 2014; Jeong et al., 2019; Li et al., 2021). Recently, 1-heptadecene-11,13-diyne-8,9,10-triol from the root of *C. japonicum* var. *ussuriense* inhibited LPS-induced NO, TNF-α, and IL-1β production in RAW 264.7 cells by inhibiting NF-κB activation (Kang et al., 2011).

### 3. Conclusions

In our current study, eight previously undescribed polyacetylenes (1–8) were obtained from the roots of *C. japonicum* var. *ussuriense*, and their chemical structures were elucidated using 1D and 2D NMR spectroscopic and the *J*-value based configuration analyses. All isolates showed inhibitory effects on LPS-induced NO production in RAW264.7 cells. The present study provides insights into the phytochemical composition of the non-polar *n*-hexane-soluble fraction of *C. japonicum* var. *ussuriense*, which is a rich source of polyacetylenes. Accordingly, polyacetylenes from *C. japonicum* var. *ussuriense* might be worthy of further investigation for their potential as anti-inflammatory agents.

## 4. Experimental

### 4.1. General experimental procedures

Optical rotations were determined using a JASCO DIP-1000 polarimeter (Jasco Co., Tokyo, Japan). UV spectra were recorded on a JASCO UV-550 spectrophotometer, and IR spectra were measured on a JASCO FT-IR 4100 spectrometer (Jasco Co., Tokyo, Japan, respectively). NMR spectra were recorded on Bruker AVANCE 400, 500, 700, 800, and 900 MHz spectrometers. HRESIMS spectra were measured on maXis 4G mass spectrometer. Column chromatography was performed using silica gel (70–230 and 230–400 mesh, Merck, Darmstadt, Germany) and Lichroprep RP-18 (40–63 μm, Merck, Darmstadt, Germany). MPLC was performed on a Biotage Isolera Prime chromatography system. Preparative HPLC was performed using a system equipped with a Waters 515 pump and 2996 photodiode-array detector and a YMC J'sphere ODS-H80 column (4 μm, 150 × 20 mm, i.d., flow rate 6 mL/min). TLC was performed using precoated silica gel 60 F<sub>254</sub> (0.25 mm, Merck, Darmstadt, Germany) plates, and the spots were detected by a 10% vanillin-H<sub>2</sub>SO<sub>4</sub> in water spray reagent.

### 4.2. Plant material

The dried roots of *Cirsium japonicum* var. *ussuriense* (Regel) Kitam. ex Ohwi (Asteraceae) (3.0 kg) were purchased from Kyungdong herbal market, Seoul, Korea, in May 2018. A voucher specimen (CBNU-2018-05-CJ) was authenticated by B. Y. Hwang and deposited at the Herbarium of the College of Pharmacy, Chungbuk National University,

Republic of Korea.

### 4.3. Extraction and isolation

The dried and powdered roots of *C. japonicum* var. *ussuriense* (3.0 kg) were extracted with MeOH (3 × 18 L) at room temperature for 3 days and then filtered. The extract was evaporated under reduced pressure, and the residue (155.0 g) was suspended in water and successively partitioned with *n*-hexane (2 × 2 L), CH<sub>2</sub>Cl<sub>2</sub> (2 × 2 L), EtOAc (2 × 2 L), and *n*-BuOH (2 × 2 L). The *n*-hexane-soluble fraction (74.0 g) was chromatographed on a silica gel column (230–400 mesh) and eluted with an *n*-hexane-EtOAc gradient system (200:1–1:1) to afford 11 fractions (CJH1 – CJH11). Fraction CJH4 (588.2 mg) was separated by MPLC using a Lichroprep RP-18 column and eluted with a MeOH–H<sub>2</sub>O gradient system (70:30–100:0) to afford 8 sub-fractions (CJH4-1 – CJH4-8). Fraction CJH4-5 (57.7 mg) was further purified by preparative HPLC (MeCN–H<sub>2</sub>O, 85:15, isocratic) to obtain compound 4 (*t*<sub>R</sub> = 30.0 min, 1.7 mg). Fraction CJH5 (1.8 g) was separated by MPLC using a Lichroprep RP-18 column and eluted with a MeOH–H<sub>2</sub>O gradient system (70:30–100:0) to provide 6 sub-fractions (CJH5-1 – CJH5-6). Fraction CJH5-2 was further purified by preparative HPLC (MeCN–H<sub>2</sub>O, 80:20, isocratic) to obtain compound 3 (*t*<sub>R</sub> = 40.0 min, 1.8 mg) and compound 8 (*t*<sub>R</sub> = 43.0 min, 2.3 mg). Fraction CJH6 (12.2 g) was chromatographed on a silica gel column (230–400 mesh) and eluted with an *n*-hexane-EtOAc gradient system (30:1 to 1:1) to afford 7 sub-fractions (CJH6-1 – CJH6-7). Fraction CJH6-6 was separated by RP-MPLC with a MeOH–H<sub>2</sub>O gradient system (60:40–100:0) to afford 10 sub-fractions (CJH6-6-1 – CJH6-6-10). Fraction CJH6-6-2 was purified by preparative HPLC (MeCN–H<sub>2</sub>O, 60:40, isocratic) to obtain compound 5 (*t*<sub>R</sub> = 36.0 min, 0.6 mg) and compound 6 (*t*<sub>R</sub> = 40.0 min, 2.3 mg). Fraction CJH6-6-3 was further purified by preparative HPLC (MeCN–H<sub>2</sub>O, 60:40, isocratic) to obtain compound 7 (*t*<sub>R</sub> = 40.0 min, 6.3 mg). The CH<sub>2</sub>Cl<sub>2</sub>-soluble fraction (23.5 g) was chromatographed on a silica gel column (230–400 mesh) and eluted with an *n*-hexane-EtOAc gradient system (30:1–1:1) to afford 9 fractions (CJC1 – CJC9). Fraction CJC8 (6.0 g) was chromatographed on a silica gel column (230–400 mesh) and eluted with a CH<sub>2</sub>Cl<sub>2</sub>–MeOH gradient system (100:1–1:1) to afford 6 sub-fractions (CJC8-1 – CJC8-6). Fraction CJC8-4 (3.0 g) was further purified by preparative HPLC (MeCN–H<sub>2</sub>O, 55:45, isocratic) to obtain compound 1 (*t*<sub>R</sub> = 30.0 min, 2.4 mg) and compound 2 (*t*<sub>R</sub> = 32.0 min, 1.2 mg).

#### 4.3.1. Cirussuryne A (1)

Brown syrup; [ $\alpha$ ]<sub>D</sub><sup>25</sup> +4 (c 0.1, MeOH); UV (MeOH)  $\lambda$ <sub>max</sub> (log  $\epsilon$ ) 213, 266, 283 nm; IR  $\nu$ <sub>max</sub> (film) 3370, 2296, 1641, 912 cm<sup>-1</sup>; <sup>1</sup>H NMR (400 MHz, CDCl<sub>3</sub>) and <sup>13</sup>C NMR (100 MHz, CDCl<sub>3</sub>), see Table 1; HRESIMS *m/z* 299.1617 [M + Na]<sup>+</sup> (calcd for C<sub>17</sub>H<sub>24</sub>NaO<sub>3</sub>, 299.1618).

#### 4.3.2. Cirussuryne B (2)

Brown syrup; [ $\alpha$ ]<sub>D</sub><sup>25</sup> +3 (c 0.1, MeOH); UV (MeOH)  $\lambda$ <sub>max</sub> (log  $\epsilon$ ) 227, 289 nm; IR  $\nu$ <sub>max</sub> (film) 3370, 2298, 1643, 910 cm<sup>-1</sup>; <sup>1</sup>H NMR (400 MHz, CDCl<sub>3</sub>) and <sup>13</sup>C NMR (100 MHz, CDCl<sub>3</sub>), see Table 1; HRESIMS *m/z* 303.1931 [M + Na]<sup>+</sup> (calcd for C<sub>17</sub>H<sub>28</sub>NaO<sub>3</sub>, 303.1931).

#### 4.3.3. Cirussuryne C (3)

Brown syrup; [ $\alpha$ ]<sub>D</sub><sup>25</sup> -4 (c 0.1, MeOH); UV (MeOH)  $\lambda$ <sub>max</sub> (log  $\epsilon$ ) 211, 270 nm; IR  $\nu$ <sub>max</sub> (film) 2298, 1745, 1643, 904 cm<sup>-1</sup>; <sup>1</sup>H NMR (900 MHz, CDCl<sub>3</sub>) and <sup>13</sup>C NMR (225 MHz, CDCl<sub>3</sub>), see Table 1; HRESIMS *m/z* 297.1828 [M + Na]<sup>+</sup> (calcd for C<sub>18</sub>H<sub>26</sub>NaO<sub>2</sub>, 297.1825).

#### 4.3.4. Cirussuryne D (4)

Brown syrup; [ $\alpha$ ]<sub>D</sub><sup>25</sup> +2 (c 0.1, MeOH); UV (MeOH)  $\lambda$ <sub>max</sub> (log  $\epsilon$ ) 214, 268, 284 nm; IR  $\nu$ <sub>max</sub> (film) 2296, 1643, 914 cm<sup>-1</sup>; <sup>1</sup>H NMR (800 MHz, CDCl<sub>3</sub>) and <sup>13</sup>C NMR (200 MHz, CDCl<sub>3</sub>), see Table 1; HRESIMS *m/z* 309.1823 [M + Na]<sup>+</sup> (calcd for C<sub>19</sub>H<sub>26</sub>NaO<sub>2</sub>, 309.1825).

#### 4.3.5. *Cirussuryne E (5)*

Brown syrup;  $[\alpha]_D^{25} +6$  (c 0.1, MeOH); UV (MeOH)  $\lambda_{\max}$  (log  $\epsilon$ ) 215, 268, 283 nm; IR  $\nu_{\max}$  (film) 3342, 2298, 1643, 896  $\text{cm}^{-1}$ ;  $^1\text{H}$  NMR (900 MHz,  $\text{CDCl}_3$ ) and  $^{13}\text{C}$  NMR (225 MHz,  $\text{CDCl}_3$ ), see Table 3; HRESIMS  $m/z$  313.1772  $[\text{M} + \text{Na}]^+$  (calcd for  $\text{C}_{18}\text{H}_{26}\text{NaO}_3$ , 313.1774).

#### 4.3.6. *Cirussuryne F (6)*

Brown syrup;  $[\alpha]_D^{25} -12$  (c 0.1, MeOH); UV (MeOH)  $\lambda_{\max}$  (log  $\epsilon$ ) 215, 268, 283 nm; IR  $\nu_{\max}$  (film) 3388, 2300, 1641, 910  $\text{cm}^{-1}$ ;  $^1\text{H}$  NMR (900 MHz,  $\text{CDCl}_3$ ) and  $^{13}\text{C}$  NMR (225 MHz,  $\text{CDCl}_3$ ), see Table 3; HRESIMS  $m/z$  313.1773  $[\text{M} + \text{Na}]^+$  (calcd for  $\text{C}_{18}\text{H}_{26}\text{NaO}_3$ , 313.1774).

#### 4.3.7. *Cirussuryne G (7)*

Brown syrup;  $[\alpha]_D^{25} +6$  (c 0.1, MeOH); UV (MeOH)  $\lambda_{\max}$  (log  $\epsilon$ ) 242 nm; IR  $\nu_{\max}$  (film) 3415, 2298, 1641, 910  $\text{cm}^{-1}$ ;  $^1\text{H}$  NMR (700 MHz,  $\text{CDCl}_3$ ) and  $^{13}\text{C}$  NMR (175 MHz,  $\text{CDCl}_3$ ), see Table 3; HRESIMS  $m/z$  315.1928  $[\text{M} + \text{Na}]^+$  (calcd for  $\text{C}_{18}\text{H}_{28}\text{NaO}_3$ , 315.1931).

#### 4.3.8. *Cirussuryne H (8)*

Brown syrup;  $[\alpha]_D^{25} +3$  (c 0.1, MeOH); UV (MeOH)  $\lambda_{\max}$  (log  $\epsilon$ ) 215, 247, 276 nm; IR  $\nu_{\max}$  (film) 2296, 1747, 1643, 912  $\text{cm}^{-1}$ ;  $^1\text{H}$  NMR (700 MHz,  $\text{CDCl}_3$ ) and  $^{13}\text{C}$  NMR (175 MHz,  $\text{CDCl}_3$ ), see Table 3; HRESIMS  $m/z$  265.1562  $[\text{M} + \text{Na}]^+$  (calcd for  $\text{C}_{17}\text{H}_{22}\text{NaO}$ , 265.1563).

#### 4.4. Measurement of LPS-induced NO production and cell viability

The RAW 264.7 macrophage cell line was obtained from ATCC (Rockville, MD, USA) and cultured in DMEM containing 5% heat-inactivated fetal bovine serum, 100 U/mL penicillin, and 100  $\mu\text{g}/\text{mL}$  streptomycin and grown at 37 °C in a humidified atmosphere containing 5%  $\text{CO}_2$ . RAW 264.7 cells were seeded into 96-well tissue culture plates at  $2 \times 10^5$  cells/mL and stimulated with 1  $\mu\text{g}/\text{mL}$  of LPS in the presence or absence of test compounds. After incubation at 37 °C for 24 h, 100  $\mu\text{L}$  of cell-free supernatant was mixed with 100  $\mu\text{L}$  of Griess reagent containing equal volumes of 2% (w/v) sulfanilamide in 5% (w/v) phosphoric acid and 0.2% (w/v) of *N*-(1-naphthyl) ethylenediamine solution to determine nitrite production. Absorbance was measured at 550 nm against a calibration curve with sodium nitrite standards. Cell viability of the remaining cells was determined by an MTT (Sigma Chemical Co., St. Louis, MO)-based colorimetric assay (Kim et al., 2021).

#### Declaration of competing interest

The authors declare that they have no known competing financial interests or personal relationships that could have appeared to influence the work reported in this paper.

#### Acknowledgements

This research was supported by the National Research Foundation of Korea (NRF) grant funded by the Korea government (MIST) (No. 2020R1A2C1008406). The authors wish to thank the Korea Basic Science Institute for the NMR spectroscopic measurements.

#### Appendix A. Supplementary material

Supplementary material to this article can be found online at <https://doi.org/10.1016/j.phytochem.2022.113319>.

#### References

- Bae, K.H., 2000. *The Medicinal Plants of Korea*. Kyohak Publishing Co., Seoul, Korea, p. 501.
- Baek, N.I., Park, J.D., Lee, Y.H., Jeong, S.Y., Kim, S.I., 1995. A novel polyacetylene from *Cirsium* spp. *Yakhak Hoeji* 39, 268–275.

- Chen, Y., Peng, S., Luo, Q., Zhang, J., Guo, Q., Zhang, Y., Chai, X., 2015. Chemical and pharmacological progress on polyacetylenes isolated from the family Apiaceae. *Chem. Biodivers.* 12, 474–502. <https://doi.org/10.1002/cbdv.201300396>.
- Christensen, L.P., 2020. Bioactive C17 and C18 acetylenic oxyliplins from terrestrial plants as potential lead compounds for anticancer drug development. *Molecules* 25, 2568. <https://doi.org/10.3390/molecules25112568>.
- Cinelli, M.A., Do, H.T., Miley, G.P., Silverman, R.B., 2020. Inducible nitric oxide synthase: regulation, structure, and inhibition. *Med. Res. Rev.* 40, 158–189. <https://doi.org/10.1002/med.21599>.
- Han, H.S., Shin, J.S., Lee, S.B., Park, J.C., Lee, K.T., 2018. Cirsimarín, a flavone glucoside from the aerial part of *Cirsium japonicum* var. *ussuriense* (Regel) Kitam. ex Ohwi, suppresses the JAK/STAT and IRF-3 signaling pathway in LPS-stimulated RAW 264.7 macrophages. *Chem. Biol. Interact.* 293, 38–47. <https://doi.org/10.1016/j.cbi.2018.07.024>.
- Jeong, D.M., Jung, H.A., Choi, J.S., 2008. Comparative antioxidant activity and HPLC profiles of some selected Korean thistles. *Arch. Pharm. Res. (Seoul)* 31, 28–33. <https://doi.org/10.1007/s12272-008-1116-7>.
- Jeong, D., Dong, G.Z., Lee, H.J., Ryu, J.H., 2019. Anti-inflammatory compounds from *Atractylodes macrocephala*. *Molecules* 24, 1859. <https://doi.org/10.3390/molecules24101859>.
- Kang, T.J., Moon, J.S., Lee, S., Yim, D., 2011. Polyacetylene compound from *Cirsium japonicum* var. *ussuriense* inhibits the LPS-induced inflammatory reaction via suppression of NF- $\kappa$ B activity in RAW 264.7 cells. *Biomol. Ther.* 19, 97–101. <https://doi.org/10.4062/biomolther.2011.19.1.097>.
- Kim, J.G., 1989. *Illustrated Natural Drugs Encyclopedia, vol. 1*. Namsandang, Seoul, Korea, p. 37.
- Kim, J.G., Lee, J.W., Le, T.P.L., Han, J.S., Kwon, H., Lee, D., Hong, J.T., Kim, Y., Lee, M.K., Hwang, B.Y., 2021. Diterpenoids and diacetylenes from the roots of *Aralia cordata* with inhibitory effects on nitric oxide production. *J. Nat. Prod.* 84, 230–238. <https://doi.org/10.1021/acs.jnatprod.0c00842>.
- Kozmiński, W., Nanz, D., 2000. Sensitivity improvement and new acquisition scheme of heteronuclear active-coupling-pattern-tilting spectroscopy. *J. Magn. Reson.* 142, 294–299. <https://doi.org/10.1006/jmre.1999.1939>.
- Kumar, S., Singh, R.K., Bhardwaj, T.R., 2017. Therapeutic role of nitric oxide as emerging molecule. *Biomed. Pharmacother.* 85, 182–201. <https://doi.org/10.1016/j.biopha.2016.11.125>.
- Lai, W.C., Wu, Y.C., Dankó, Cheng, Y.B., Hsieh, T.J., Hsieh, C.T., Tsai, Y.C., El-Shazly, M., Martins, A., Hohmann, J., Hunyadi, A., Chang, F.R., 2014. Bioactive constituents of *Cirsium japonicum* var. *asutrale*. *J. Nat. Prod.* 77, 1624–1631. <https://doi.org/10.1021/np500233t>.
- Li, X.R., Liu, J., Peng, C., Zhou, Q.M., Liu, F., Guo, L., Xiong, L., 2021. Polyacetylene glucosides from the florets of *Carthamus tinctorius* and their anti-inflammatory activity. *Phytochemistry* 187, 112770. <https://doi.org/10.1016/j.phytochem.2021.112770>.
- Matsumori, N., Kaneno, D., Murata, M., Nakamura, H., Tachibana, K., 1999. Stereochemical determination of acyclic structures based on carbon–proton spin-coupling constants. A method of configuration analysis for natural products. *J. Org. Chem.* 64, 866–876. <https://doi.org/10.1021/jo981810k>.
- Menche, D., 2008. New methods for stereochemical determination of complex polyketides: configurational assignment of novel metabolites from myxobacteria. *Nat. Prod. Rep.* 25, 905–918. <https://doi.org/10.1039/B707989N>.
- Negri, R., 2015. Polyacetylenes from terrestrial plants and fungi: recent phytochemical and biological advances. *Fitoterapia* 106, 92–109. <https://doi.org/10.1016/j.fitote.2015.08.011>.
- Park, J.C., Hur, J.M., Park, J.G., Kim, S.C., Park, J.R., Choi, S.H., Choi, J.W., 2004. Effects of methanol extract of *Cirsium japonicum* var. *ussuriense* and its principle, hispidulin-7-O-neohesperidose on hepatic alcohol-metabolizing enzymes and lipid peroxidation in ethanol-treated rats. *Phytother. Res.* 18, 19–24. <https://doi.org/10.1002/ptr.1299>.
- Park, J.C., Yoo, H., Kim, C.E., Shim, S.Y., Lee, M., 2017. Hispidulin-7-O-neohesperidose from *Cirsium japonicum* var. *ussuriense* attenuates the production of inflammatory mediators in LPS-induced RAW 264.7 cells and HT-29 cells. *Phcog. Mag.* 13, 707–711. <https://doi.org/10.4103/0973-1296.218116>.
- Shim, H., Moon, J.S., Lee, S., Yim, D., Kang, T.J., 2012. Polyacetylene compound from *Cirsium japonicum* var. *ussuriense* inhibited caspase-1-mediated IL-1 $\beta$  expression. *Immun. Netw.* 12, 213–216. <https://doi.org/10.4110/in.2012.12.5.213>.
- Takaishi, Y., Okuyama, T., Masuda, A., Nakano, K., Murakami, K., Tomimatsu, T., 1990. Acetylenes from *Cirsium japonicum*. *Phytochemistry* 29, 3849–3852. [https://doi.org/10.1016/0031-9422\(90\)85345-G](https://doi.org/10.1016/0031-9422(90)85345-G).
- Takaishi, Y., Okuyama, T., Nakano, K., Murakami, K., Tomimatsu, T., 1991. Absolute configuration of a triolacetylene from *Cirsium japonicum*. *Phytochemistry* 30, 2321–2324. [https://doi.org/10.1016/0031-9422\(91\)83640-7](https://doi.org/10.1016/0031-9422(91)83640-7).
- Thao, N.T., Cuong, T.D., Hung, T.M., Lee, J.H., Na, M., Son, J.K., Jung, H.J., Fang, Z., Woo, M.H., Choi, J.S., Min, B.S., 2011. Simultaneous determination of bioactive flavonoids in some selected Korean thistles by high-performance liquid chromatography. *Arch. Pharm. Res. (Seoul)* 34, 455–461. <https://doi.org/10.1007/s12272-011-0314-x>.
- Tsukamoto, S., Kato, H., Hirota, H., Fusetani, N., 1997. Seven new polyacetylene derivatives, showing both potent metamorphosis-inducing activity in ascidian larvae and antifouling activity against barnacle larvae, from the marine sponge *Callyspongia truncata*. *J. Nat. Prod.* 60, 126–130. <https://doi.org/10.1021/np9606097>.
- Wavefunction Inc., 2013. *Spartan '14* (Irvine, CA, USA).
- Yao, C.M., Yang, X.W., 2014. Bioactivity-guided isolation of polyacetylenes with inhibitory activity against NO production in LPS-activated RAW264.7 macrophages from the rhizomes of *Atractylodes macrocephala*. *J. Ethnopharmacol.* 151, 791–799. <https://doi.org/10.1016/j.jep.2013.10.005>.